We are IntechOpen, the world's leading publisher of Open Access books Built by scientists, for scientists

4,800
Open access books available

122,000
International authors and editors

135M
Downloads

Our authors are among the

154
Countries delivered to

TOP 1%
most cited scientists

12.2%
Contributors from top 500 universities

WEB OF SCIENCE™

Selection of our books indexed in the Book Citation Index in Web of Science™ Core Collection (BKCI)

Interested in publishing with us?
Contact book.department@intechopen.com

Numbers displayed above are based on latest data collected.
For more information visit www.intechopen.com

12

In-Situ Structural Characterization of SWCNTs in Dispersion

Zhiwei Xiao, Sida Luo and Tao Liu
Florida State University
United States

1. Introduction

Owing to its excellent mechanical robustness – high strength, stiffness, toughness (Saito et al., 1998; Baughman et al., 2002), excellent electrical and thermal conductivity and piezoresistivity (Cao et al., 2003; Grow et al., 2005; Skakalova et al., 2006), and versatile spectroscopic and optoelectronic properties (Burghard, 2005; Dresselhaus et al., 2005; Dresselhaus et al., 2007; Avouris et al., 2008), single-walled carbon nanotubes (SWCNTs) offer a great promise as the building blocks for the development of multi-functional nanocomposites (Hussain et al., 2006; Moniruzzaman & Winey, 2006; Green et al., 2009; Chou et al., 2010; Sahoo et al., 2010). To fabricate the SWCNT based multi-functional nanocomposites, one of the most used approaches is through solution or melt processing of SWCNT dispersions in various polymer matrices (Hilding et al., 2003; Moniruzzaman & Winey, 2006; Schaefer & Justice, 2007; Grady, 2009). In addition, the SWCNT dispersions in different liquid media of small molecules, e.g., water or organic solvents, were also proved to be useful for cost-effective processing of SWCNT thin film based novel applications (Cao & Rogers, 2009), e.g., CNT film strain sensors (Li et al., 2004), high mobility CNT thin film transistors (Snow et al., 2005), SWNT thin film field effect electron sources (Bonard et al., 1998) and various CNT film-based transparent electronics (Gruner, 2006). To fully explore the use of SWCNT dispersions for various technologically important applications, it is critical to have a good understanding of the processing-structure relationship of SWCNT dispersions processed by different techniques and methods (Luo et al., 2010).

Regardless of the dispersion processing methods, it has been recognized that, to disperse SWCNTs at a molecular level in either small molecule solvent or polymer solution or melt is extremely difficult (Moniruzzaman & Winey, 2006; Schaefer & Justice, 2007; Mac Kernan & Blau, 2008). The fundamental reasons for such difficulties are threefold. First, the one dimensional tubular structure of SWCNTs imparts this novel species of very high rigidity. When mixed with the solvent of small molecules or flexible chain polymers, the highly rigid nature of SWCNTs as well as its long aspect ratio character (typically >100) results in a competition between the orientational entropy and the packing entropy that drives the mixture towards phase separation (Onsager, 1949; Flory, 1978; Fakhri et al., 2009). The persistence length is a physical measure of the rigidity of a chain-like or worm-like molecule (Tracy & Pecora, 1992; Teraoka, 2002). Depending upon the tube diameter, the theoretically estimated persistence length for an individual SWCNT is as high as of 30 – 1000 μm (Yakobson & Couchman, 2006). This result has been confirmed by the experimental studies

of SWCNT dynamics in aqueous suspension (Duggal & Pasquali, 2006; Fakhri et al., 2009). For comparison, the persistence length of a few widely studied stiff particles/molecules is: 300 nm for the tobacco mosaic virus (TMV), 80 nm for poly (γ-benzyl L-glutamate) (PBLG), and 50 nm for double-stranded DNA (Vroege & Lekkerkerker, 1992). Second, the intertube van der Waals interaction of SWCNTs is very strong. The cohesive energy for a pair of parallel arranged SWCNTs at equilibrium is greater than 2.0 eV/nm (Girifalco et al., 2000). For this reason, one often finds that the SWCNTs organize into a rope or bundle structure in the as-produced materials (Thess et al., 1996; Salvetat et al., 1999). To disperse SWCNTs in a given medium at the molecular level or to exfoliate the SWCNT bundles into individual tubes, the strong intertube cohesive energy has to be overcome. This proved to be a difficult task (O'Connell et al., 2002; Islam et al., 2003; Moore et al., 2003; Zheng et al., 2003; Cotiuga et al., 2006; Giordani et al., 2006; Bergin et al., 2007; Liu et al., 2007; Liu et al., 2009). Lastly, the difficulty to disperse SWCNTs is also attributed to the topological entanglement or enmeshment of long aspect ratio SWCNTs, which could result kinetically quenched fractal structures or aggregates.

Associated with the threefold difficulty to disperse SWCNTs is their hierarchical structures that one may encounter in the dispersion. As schematically shown in Fig. 1, these structures include: 1) the individual tubes with different molecular structure as specified by the rolling or chiral vector (n, m) (Saito et al., 1998); 2) the SWCNT bundles that is composed of multiple individual tubes approximately organized into a 2D hexagonal lattice with their long axis parallel to each other (Thess et al., 1996; Salvetat et al., 1999); 3) the SWCNT aggregates formed by the topological entanglement or enmeshment of individual tubes and/or SWCNT bundles; and 4) the SWCNT networks that span the entire dispersion sample, which may occur as a result of inter-tube, inter-bundle and inter-aggregate connection when the SWCNT loading in the dispersion is high. In a given SWCNT dispersion, the diameter and length of the individual tubes and the SWCNT bundles, the radius of gyration of the SWCNT aggregates, as well as the relative amount of the hierarchical structures of the SWCNTs could be subject to random variations. This brings out the length-scale related polydispersity issues. The length scales of the hierarchical SWCNT structures vary from ~ 10^0 nm for the diameter of individual tube, ~10^1 nm for the diameter of SWCNT bundles, ~ 10^2 – 10^3 nm for the length of SWCNT tubes and bundles, ~10^4 – 10^5 nm for the size of SWCNT aggregates, and up to the macroscopic sample size for the SWCNT networks. Given such a broad range of length scales involved in the hierarchical structures of SWCNTs possibly encountered in the dispersion, one can expect that, to quantitatively characterize the structures of SWCNT dispersion and establish the related dispersion processing-structure relationship, a multi-scale characterization approach should be utilized.

The past decades witnessed significant progress being made toward qualitative and quantitative characterization of the SWCNT dispersions by various experimental techniques. Among the different techniques, the microscopy based methods, e.g., optical microscopy (OM), electron microscopy (SEM and TEM) and atomic force microscopy (AFM), have been routinely used for characterizing the SWCNT structures to provide valuable information regarding the diameter, length, and the overall morphology for a given SWCNT sample. However, when applied to characterizing the SWCNT dispersions, the microscopy techniques typically require a sample preparation protocol that converts the dispersion sample from a liquid state to solid state. This may cause the structural changes of the SWCNTs during the sample preparation and thus fail to faithfully provide the desired

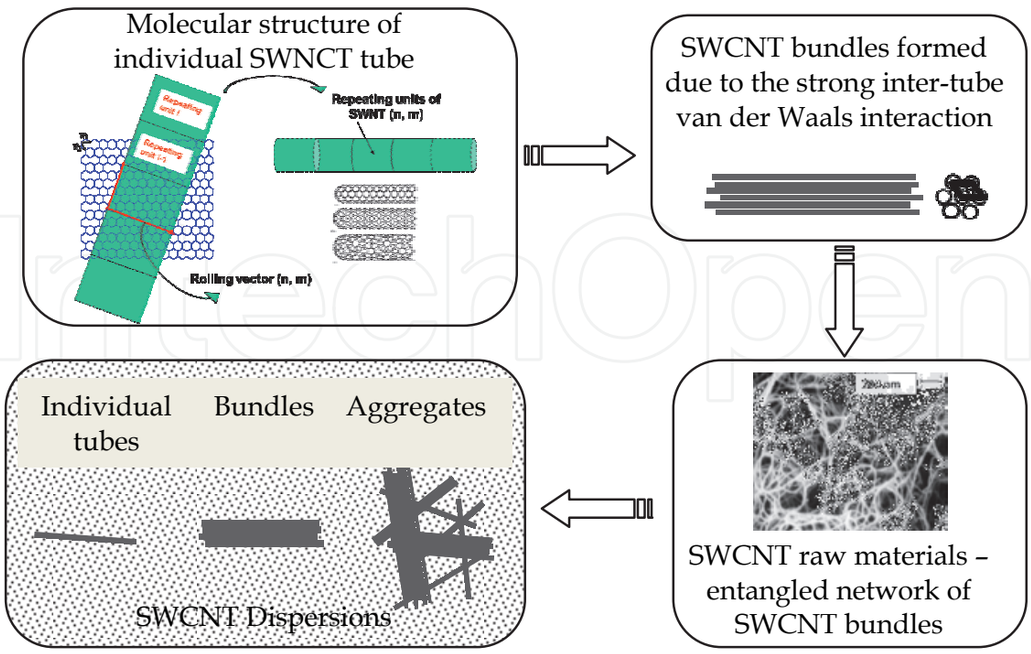

Fig. 1. Schematic SWCNT structures at different length scales

in-situ structural information of the SWCNTs in the dispersion. For this reason, the microscopy technique will not be considered as suitable methods for in-situ structural characterization of SWCNT dispersions. In addition to the microscopy techniques, a few other conventional or non-conventional techniques emerge to show great promise for the in-situ structural characterization of SWCNT dispersions. These emerging techniques include:

1. Viscosity and rheological measurements;
2. Scattering based techniques, e.g., elastic and quasi-elastic light scattering (SLS and DLS), small-angle X-ray and neutron scattering (SAXS and SANS);
3. Sedimentation methods, e.g., analytical and preparative ultracentrifuge method; and
4. Spectroscopic techniques, e.g., simultaneous Raman scattering and photoluminescence spectroscopy.

To facilitate a multi-scale characterization approach for a better understanding of the in-situ SWCNT structures in the dispersion, the above listed experimental techniques and methods will be reviewed in this chapter. For each of the methods, the underlying physical principles and their applications for the in-situ structural characterization of SWCNT dispersions are discussed in the subsequent sections.

2. Viscosity and rheological measurements

Suspensions or dispersions, in which the microscopically visible solid particles or fillers are dispersed in a continuous phase like water, organic solvent or polymer solutions, find themselves a great technical importance in many different areas, e.g., biotechnology, cement and concrete technology, ceramic processing, coating and pigment technology, etc. The rheological behavior of a two-phase suspension system has received a great attention and been studied for many years (Batchelor, 1974; Jeffrey & Acrivos, 1976; Russel, 1980; Metzner, 1985; Bicerano et al., 1999; Hornsby, 1999; Larson, 1999; Petrie, 1999). One area concerning

the rheological behavior of a suspension system is to understand the shear viscosity of a suspension. To this effect, hundreds of empirical, semi-empirical, and theoretical relationships have been developed for relating the dispersion viscosity, η, with respect to the volume fraction, the shape of the fillers, and the shear rate under which the viscosity is measured (Bicerano et al., 1999; Hornsby, 1999; Shenoy, 1999). At very low filler volume fraction and zero shear rate, the viscosity η of a suspension or dispersion is given by:

$$\frac{\eta}{\eta_0} \approx 1 + [\eta]\varphi \tag{1}$$

where η_0 is the viscosity of the liquid medium, ϕ is the volume fraction of the fillers, and $[\eta]$ is termed as the intrinsic viscosity and it is a dimensionless, scale-invariant functional of the shape of the filler particle. By applying the numerical path integration technique, Douglas et al (Mansfield & Douglas, 2008) presented an accurate expression for the intrinsic viscosity of cylinders applicable to a broad range of aspect ratios ($2.72 < A < \infty$), which is:

$$[\eta] = \frac{8A^2}{45}\left[\ln\left(\frac{4A}{e^{25/12}}\right)\right]^{-1} \times \left[\frac{1 - 1.178t + 1.233t^{1.86} + 1.925t^{6.28} + 0.625t^{12.67}}{1 - 1.094t + 0.757t^{3.83} + 1.344t^{3.83} + 1.978t^{12.07}}\right] \tag{2a}$$

$$A = \frac{L}{d} \tag{2b}$$

$$t = \frac{1}{\ln A} \tag{2c}$$

where A is the aspect ratio of the cylinder and equals to the ratio of the cylinder length L to its diameter d. By taking advantage of the rigid rod nature of SWCNTs (Yakobson & Couchman, 2006; Duggal & Pasquali, 2006; Fakhri et al., 2009) and on the basis of Eq. (1) and (2), the aspect ratio of SWCNTs in the dispersion might be determined by the viscosity measurement technique, e.g., the steady-state simple shear experiments.

By following this line of thought, a few studies were carried out for determining the aspect ratio of SWCNT particles in superacid (Davis et al., 2004) and aqueous dispersions (Parra-Vasquez et al., 2007), where the volume fraction of SWCNTs is a few factor of 10^{-5}. The experimentally determined intrinsic viscosity of SWCNTs in superacid (8300 ± 830) and in aqueous dispersion (7350 ± 750) respectively lead to the estimated aspect ratio of SWCNTs to be 470 ± 30 and 505 ± 35. The similar and very large aspect ratio of the SWCNTs in these two distinctly different dispersion systems indicate the dominant structures of SWCNTs in the dispersion are the individual tubes and/or the SWCNT bundles. It is noted that, the intrinsic viscosity relationship used in these studies is based on a formula given by Batchelor (Batchelor, 1974), which is:

$$[\eta] = \frac{8A^2}{45}\varepsilon \times \left[\frac{1 + 0.64\varepsilon}{1 - 1.5\varepsilon} + 1.659\varepsilon^2\right] \tag{3a}$$

$$\varepsilon = \frac{1}{\ln 2A} \tag{3b}$$

When compared to the accurate expression given by Eq. (2) (Mansfield & Douglas, 2008), the relationship given by Eq. (3) overestimates the intrinsic viscosity by 12% or more for the rods with aspect ratio below 100.

In order to appropriately use Eq. (1) and (2) for estimating the aspect ratio of SWCNTs in the dispersion, the volume fraction of the filler particles has to be kept low. In addition to this requirement, the viscosity measurements also need to be done at a relatively low shear rate. Otherwise, the slender particles with large aspect ratio, e.g., SWCNTs, can be aligned along the flow direction to cause the shear-thinning effect and thus result in a shear-rate dependent intrinsic viscosity, which is not taken into account by Eq. (1) and (2). The Peclet number (Bicerano et al., 1999; Larson, 1999) (*Pe*), defined by the ratio of the characteristic experimental shear rate to the rotational diffusion coefficient of the filler particle,

$$Pe = \frac{\dot{\gamma}}{D_r} \tag{4a}$$

$$D_r = \frac{3k_BT}{\pi\eta_0 L^3}\left(\ln A + 2\ln 2 - \frac{11}{6}\right) \tag{4b}$$

$$D_t = \frac{k_BT}{3\pi\eta_0 L}\left(\ln A + 2\ln 2 - 1\right) \tag{4c}$$

can be used as a criterion to select appropriate experimental conditions to avoid the complication caused by the shear-thinning effect. When *Pe* is smaller than 1, the rotational Brownian motion of the slender particle is able to overcome the shear-field induced alignment and randomize the particle orientation to minimize the shear-thinning effect. In Eq. (4), k_B is the Boltzmann constant and T is the temperature. The rotational and translational diffusion coefficient, D_r and D_t, is taken from the work by Bonet Avalos (Avalos et al., 1993) and Yamakawa (Yamakawa, 1975). D_t is given here for completeness and convenience and will be used for a later discussion on the dynamic light scattering technique for characterizing the SWCNT structures.

The steady-state simple shear experiments for the SWCNT dispersion at relatively low particle volume fraction allow one to determine the intrinsic viscosity of SWCNTs and thus infer the particle aspect ratio. In addition to this, the unsteady-state simple shear experiments, e.g., small-amplitude oscillatory flow, also enable one to study the viscoelastic behavior of SWCNT dispersions at relatively high particle volume fraction. Hough et al. (Hough et al., 2004) investigated the dynamic mechanical properties of SWCNT aqueous dispersions with particle volume fraction greater than 10^{-3}. The observed oscillation frequency independent storage modulus G' and loss modulus G'' allow the author to infer the presence of SWCNT network structures in the dispersion. The network structure is formed by the physical association of the SWCNT rods, and the bonding energy responsible for the association is as high as ~ 40 k_BT. The similar viscoelastic behavior studies were performed for the SWCNT dispersion in epoxy (Ma et al., 2009) and in unsaturated polyester (Kayatin & Davis, 2009). These polymeric resin based dispersion system presents a strong elastic response at relatively high volume fraction of SWCNTs, which also signifies the formation of SWCNT networks.

In brief, the viscosity and rheological measurements are capable of providing the in-situ structural information of SWCNTs in different dispersing media. The SWCNT structures

being probed include the aspect ratio of the individual tubes or SWCNT bundles as well as the network formation of SWCNTs.

3. Scattering techniques

For a long time, the elastic scattering techniques, e.g., static light scattering (SLS), small angle X-ray (SAXS) and neutron scattering (SANS) have been widely used for obtaining the structural information of materials of many kinds (Guinier & Fournet, 1955; Glatter & Kratky, 1982; Feigin & Svergun, 1987; Chu, 1991; Higgins & Benoit, 1994). In a typical elastic scattering experiment, a collimated beam of probe particles, e.g., photons in SLS and SAXS, neutrons in SANS, interacts with a sample system that is composed of many scattering units or scatterers. The interaction between the probe beam and the scatterer at position $\vec{r}_i$ produces a spherical scattered wave propagating outwardly from $\vec{r}_i$ toward the detector. The scattering beam intensity recorded by the detector, I_D, is a result of the superposition of the multiple spherical scattered waves originated from the many scatterers that are bathed in an illuminated volume V defined by the incident probe beam and the detection optics. I_D is related to the differential scattering cross section $d\sigma/d\Omega$ and given by (Graessley, 2004):

$$\frac{d\sigma}{d\Omega} = \frac{I_D r_D^2}{V I_0} = \sum_{j=1}^{n}\sum_{k=1}^{n} b_j b_k \exp\left[i\vec{q}\cdot\left(\vec{r}_j - \vec{r}_k\right)\right] \tag{5a}$$

$$\vec{q} = \frac{2\pi}{\lambda}\left(\vec{s}_0 - \vec{s}_D\right) \tag{5b}$$

$$q = \left|\vec{q}\right| = \frac{4\pi}{\lambda}\sin\frac{\theta}{2} \tag{5c}$$

Normalized by the incident flux of the probe particles, which is the number of the particles impinging on a unit area of the sample per unit time, the differential scattering cross-section $d\sigma/d\Omega$ is defined as the number of scattered particles generated per unit time per unit volume of the sample within a unit solid angle subtended by the detector. In Eq. (5), b_j is the scattering length of the scatterer j, a quantity to measure the scattering power of a given species that depends on the details of the probe/scatterer interaction; I_0 is the incident beam intensity; r_D is the distance from the scatterer to the detector; $\vec{q}$ is the scattering vector and defined by the difference between the propagation vector of the incident beam ($2\pi\,\vec{s}_0\,/\lambda$) and that of the scattered beam ($2\pi\,\vec{s}_D\,/\lambda$); the scattering angle formed by the incident beam and the scattered beam is θ; and λ is the wavelength of the incident beam. As noted in Eq. (5), the scattered beam intensity contains the relative spatial position ($\vec{r}_j$ - $\vec{r}_k$) of the scatterers, which forms the basis of using the elastic scattering techniques for characterizing the structures of suspension or dispersions. For a dispersion system of monodispersed particles with random orientation, the generalized differential scattering cross section given by Eq. (5a) can be simplified to (Ballauff et al., 1996; Pedersen, 1997; Peterlik & Fratzl, 2006):

$$\frac{d\sigma}{d\Omega} = n\Delta\rho^2 \upsilon^2 P(q) S(q) \tag{6}$$

where n is the number density of the particles; $\Delta\rho$ is the difference in scattering length density (scattering length per unit volume of the dispersion particle) between the particles and the dispersing medium; v is the volume of the particle; $P(q)$ is the particle form factor due to the intra-particle contribution to the scattering and characterizes the particle size and shape; and $S(q)$ is the structure factor to reflect the inter-particle contribution to the scattering, which characterizes the relative positions of different particles and contains the interaction information between the particles. Owing to the difficulties of separating the inter- and intra-particle contributions to the dispersion structure, the scattering experiments are usually carried out for dilute dispersion system to minimize the inter-particle contribution. In this case, the structure factor $S(q) = 1$. Without introducing the complication of the inter-particle contribution, the size and shape of the particles in a dilute dispersion can be determined by fitting the scattering intensity with Eq. (6) by applying appropriate form factor $P(q)$. Pedersen (Pedersen, 1997) summarized 27 different form factors, a few of which relevant to the structural characterization of SWCNT dispersions are given below:

1. Form factor for cylinder of length L and radius R

$$P_1(q) = \int_0^{\pi/2} \left[\frac{2J_1(qR\sin\alpha)}{qR\sin\alpha} \frac{\sin\left[(qL\cos\alpha)/2\right]}{(qL\cos\alpha)/2} \right]^2 \sin\alpha d\alpha \tag{7}$$

where $J_1(x)$ is the Bessel function of the first kind of order one.

2. Form factor for flexible polymer chain

$$P_2(q) = \frac{2\left[\exp(-q^2 R_g{}^2) + q^2 R_g{}^2 - 1\right]}{\left(q^2 R_g{}^2\right)^2} \tag{8}$$

where R_g^2 is the mean squared radius of gyration of a Gaussian chain and equals to $(L_c l_k)/6$. L_c is the contour length and l_k is the Kuhn step length of the polymer chain.

3. Form factor for cylinder of length L and radius R with attached N_c Gaussian chains of contour length L_c

$$P_3(q) = \frac{1}{\left(\rho + N_c\rho_c\right)^2}\left[\rho^2 P_1(q) + N_c\rho_c^2 P_2(q) + N_c(N_c-1)\rho_c^2 S_1(q) + 2N_c\rho\rho_c S_2(q)\right] \tag{9a}$$

$$S_1(q) = \left[\frac{1-\exp(-q^2 R_g{}^2)}{q^2 R_g{}^2}\right]^2 \times \int_0^{\pi/2} \left\{2J_0(qR\sin\alpha)\cos\left[(qL\cos\alpha)/2\right]\right\}^2 \sin\alpha d\alpha \tag{9b}$$

$$S_2(q) = \left[\frac{1-\exp(-q^2 R_g{}^2)}{q^2 R_g{}^2}\right] \times \int_0^{\pi/2} \frac{2J_1(qR\sin\alpha)}{qR\sin\alpha} \frac{\sin\left[(qL\cos\alpha)/2\right]}{(qL\cos\alpha)/2} 2J_0(qR\sin\alpha) \cos\left[(qL\cos\alpha)/2\right]\sin\alpha d\alpha \tag{9c}$$

where $J_0(x)$ is the Bessel function of the first kind of order zero; ρ and ρ_c is respectively the total excess scattering length of the cylinder and the polymer chains.

Dror (Dror et al., 2005), Yurekli et al. (Yurekli et al., 2004) and Granite et al. (Granite et al., 2010) respectively investigated the structures of styrene-sodium mealeate copolymer and

gum arabic wrapped, SDS–stabilized, and pluronic copolymer dispersed SWCNT dispersions by SANS technique. All these studies indicated that the dispersing agents, either the ionic surfactant SDS or the copolymers being used, adsorbed on the SWCNTs to form a core-shell structure, in which the core is formed by thin SWCNT bundles and the shell is attributed to the physical adsorption of the dispersing agents. With the refined cylindrical core-shell form factors, the diameter of the core and the thickness of the shell have been determined by fitting the experimentally determined SANS scattering intensity. It is particularly interesting to note that, for the SDS-stabilized SWCNT dispersions, the SANS experiments indicated that, within the shell, the SDS surfactant molecules do not form any ordered micelle structures but are randomly distributed (Yurekli et al., 2004). One recent molecular dynamic simulation study on the SDS aggregation on SWCNTs (Tummala & Striolo, 2009) supports such a viewpoint. However, another MD simulation study (Xu et al., 2010) reveals a much delicate situation for the SDS structure formation on SWCNTs. Depending upon the diameter of SWCNT as well as the coverage density, the SDS molecules can organize into cylinder-like monolayer structure, hemicylindrical aggregates, and randomly organized structures on the surface of a SWCNT. It is expected that the combined simulation and scattering experiments could ultimately help to have a better understanding of this interesting phenomena.

In addition to the above described form-factor modeling approach, another commonly used method for understanding, analyzing and interpreting the small-angle scattering data is by a much simpler and physically appealing scaling approach (Oh & Sorensen, 1999; Sorensen, 2001). The scaling approach is based on a comparison of the inherent length scale of the scattering, *1/q*, and the length scales in the system of scatterers to qualitatively understand the behaviors of the differential scattering cross section in relation to the structures of the scattering system. Two limiting situations can be used for illustrating the principle of the scaling approach. When the *n* scatterers are within a *1/q* distance from each other, the phase of the *n* scattered waves will be in phase and $\vec{q}\cdot\left(\vec{r}_j-\vec{r}_k\right)<1$. In this case, the double sum in Eq. (5a) equals to n^2. On the other hand, when the *n* scatterers are separated from each other by a distance greater than *1/q*, the phase of the *n* scattered waves will be random and $\vec{q}\cdot\left(\vec{r}_j-\vec{r}_k\right)>1$. In such a case, the double sum in Eq. (5a) equals to *n*. With these results and bear in mind that, for a finite-sized scattering system with uniformly distributed scatterers, the non-zero scattering contribution at a scattering angle other than zero is due to the scatterer density fluctuation on the surface, one can derive a power-law relationship for the scattering intensity of a fractal aggregate with respect to the inherent length scale of *1/q* (Xu et al., 2010). It is stated as:

$$\frac{d\sigma}{d\Omega}\propto I_D\propto n^2(qR_g)^{-D}\quad for\quad a<1/q<R_g \tag{10}$$

where *D* is the fractal dimension of an aggregate system. For a homogeneous 1D rod, *D* = 1; 2D disk, *D* = 2; and 3D sphere, *D* = 3. Eq. (10) applies to a fractal aggregate system defined by two length scales: *a* is the size of the scatterer and R_g is the radius gyration of the aggregate. The scaling approach makes the physical significance of the inherent length scale *1/q* more transparent and easier to comprehend.

With the help of Eq. (10), the fractal structures of SWCNTs in the dispersion have been investigated by SAXS (Schaefer et al., 2003a; 2003b), SANS (Zhou et al., 2004; Wang et al.,

2005; Bauer et al., 2006; Hough et al., 2006; Urbina et al., 2008) and SLS (Chen et al., 2004). Depending upon the sample preparation conditions, both the rigid-rod structure of SWCNTs (with D = 1) and the entangled SWCNT fractal networks (2 < D < 3) have been observed. It is noted that, among the different scattering techniques being used for characterizing the SWCNT structures in different types of dispersions, the SANS was more popular than the others. This is partially attributed to the relatively high scattering contrast ($\Delta\rho$) of SWCNTs when interact with neutron as compared to X-rays. In addition, the strong optical absorption of SWCNTs in the visible light region could potentially complicate the SLS experiments and make the data interpretation and analysis more difficult. The experimental difficulties related to the SLS technique for the structural characterization of SWCNT dispersions has not been given sufficient attention.

The scattering experiments introduced above rely on measuring the time-averaged scattering intensity as a function of the scattering vector for characterizing the dispersion structures. In addition to this approach, another type of scattering experiments, e.g., dynamic light scattering (DLS) or quasi-elastic light scattering (Chu, 1991; Berne & Pecora, 2000; Teraoka, 2002), is also a valuable technique for in-situ characterizing the dispersion structures. The DLS method takes measurements of the time fluctuation of the scattered beam intensity to determine the time-dependent correlation function of a dynamic system, which provides a concise way for describing the degree to which two dynamic properties are correlated over a period of time. In DLS experiments, the normalized time correlation functions, $g_2(\tau)$, of the scattered light intensity is recorded and given by:

$$g_2(\tau) = \frac{< I_D(t) I_D(t+\tau) >}{< I_D(t) I_D(t) >} \tag{11}$$

which is related to the time correlation function, $g_1(\tau)$, of the scattered electric field (E_D)

$$g_1(\tau) = \frac{< E_D(t) E_D(t+\tau) >}{< E_D(t) E_D(t) >} \tag{12}$$

by

$$g_2(\tau) = 1 + \gamma \left[g_1(\tau) \right]^2 \tag{13}$$

where γ is a constant determined by the specific experiment setup. Both polarized and depolarized DLS experiments can be performed. In the former (latter) experiments, the incident beam is in a vertical polarization direction and the vertically (horizontally) polarized scattered light is detected. Depending upon whether a polarized or depolarized DLS experiment is performed, for a dilute dispersion of rodlike particles, $g_1(\tau)$, is related to the distribution of the diffusion coefficients of the particles by (Chu, 1991; Berne & Pecora, 2000; Lehner et al., 2000; Shetty et al., 2009) :

$$\left| g_1(\tau) \right| = \int G(\Gamma) \exp(-\Gamma \tau) d\Gamma \tag{14a}$$

$$\Gamma = D_t q^2 + 6 D_r \text{ for depolarized DLS} \tag{14b}$$

$$\Gamma = D_t q^2 \text{ for polarized DLS} \tag{14c}$$

where $G(I)$ is a distribution function to characterize the polydispersity of the particles; D_t and D_r are respectively the translational and rotational diffusion coefficients of the rods. Upon determination of the rotational and translational diffusion coefficient by the depolarized DLS measurements, one can solve the system equation of Eq. (4b) and (4c) to obtain the length and diameter of the rods. With this approach, Shetty et al (Shetty et al., 2009) and Badaire et al (Badaire et al., 2004) respectively investigated using the polarized DLS technique for in-situ determination of the average length and diameter of functionalized SWCNTs as well as SDS-stabilized SWCNTs in aqueous dispersions. Similar to SLS technique, the strong optical absorption of SWCNTs could also cause the experimental difficulties in using the DLS technique for the structural characterization of SWCNT dispersions.

4. Sedimentation characterization techniques

Analytical ultracentrifugation is a powerful and well-known technique in the areas of biochemistry, molecular biology and macromolecular science for characterizing the sedimentation, diffusion behaviors and the molecular weights of both synthetic and natural macromolecules (Fujita, 1975; Laue & Stafford, 1999; Colfen & Volkel, 2004; Brown & Schuck, 2006). The preparative ultracentrifuge also found applications on the characterization of proteins (Shiragami & Kajiuchi, 1990; Shiragami et al., 1990) and macromolecules (Pollet et al., 1979). Fig. 2 schematically shows the operational principle of the ultracentrifugation technique for characterizing the dispersion structures. When the dispersion is subject to centrifugation, the centrifugal force and the thermal agitation respectively cause gravitational drift and Brownian motion of the small particles in the dispersion. As a result, the originally uniformly distributed small particles with concentration of C_0 will develop into a certain concentration profile $C(r, t)$ at a given time t. The governing equation for describing the particle concentration profile can be derived on the basis of mass balance (Mason & Weaver, 1926; Waugh & Yphantis, 1953; Fujita, 1975; Shiragami & Kajiuchi, 1990) and given by:

$$\frac{\partial C}{\partial t} = D\left(\frac{\partial^2 C}{\partial r^2}\right) - s\omega^2 r_m \frac{\partial C}{\partial r}$$

$$\begin{aligned} &C = C_0 \qquad (t = 0) \\ &D\frac{\partial C}{\partial r} = s\omega^2 r_m C \qquad r = r_1, \quad r = r_2; \quad t > 0 \\ &r_m = \frac{r_1 + r_2}{2} \end{aligned} \tag{15}$$

where s and D are respectively the sedimentation and translational diffusion coefficient of the particles. For rodlike particles, the relationship between D and its geometric dimension is given by Eq. (4c); and s is given by:

$$s = \frac{m(1 - v\rho_0)}{3\pi\eta_0 L}(\ln A + 2\ln 2 - 1) \tag{16}$$

In Eq. (16), m is the mass of the particle; ν is its partial specific volume and can be approximated by the reciprocal of the particle mass density; and ρ_0 is the density of the liquid media.

An approximation is implied in Eq. (15). That is, irrespective of its distance from the center of rotation, the centrifugal field experienced by the particle is uniform and given by $\omega^2 r_m$. With this approximation, Eq. (15) can be solved analytically and the solution can be found in the cited references. With the analytical ultracentrifuge instrument, one can experimentally measure the concentration profile of the dispersion at a given set of centrifugation conditions. Upon fitting the theoretically predicted concentration profile given by Eq. (15), the transport properties, s and D, of the particle can be determined, from which the structural information of the particle can be inferred. The analytical ultracentrifuge has recently been reported as a methodology for rapid characterization of the quality of carbon nanotube dispersions (Azoubel & Magdassi, 2010). Nevertheless, no efforts have been pursued for quantitatively extracting the structural information of the carbon nanotube dispersions being studied in this work.

In addition to the analytical ultracentrifuge approach, another sedimentation measurement based characterization technique - preparative ultracentrifuge method (PUM) (Liu et al., 2008) has been recently developed by the authors. The PUM method relies on measuring and analyzing the sedimentation function of a given SWCNT dispersion for quantitative characterizing the transport properties and the structures of SWCNTs. The idea to define the sedimentation function is schematically shown in Fig. 2 and described as follows: when a certain amount of dispersion is subject to centrifugation, the number of particles, $N(V, t=0)$, in a given control volume V before centrifugation will decrease to $N(V, t)$ after time t. The sedimentation function is given by the ratio of $N(V, t)$ to $N(V, t=0)$ and related to the particle concentration profile $C(r, t)$ by:

$$F_p(t;s,D,\omega,G,r_1,r_2)=\frac{N(V,t)}{N(V,t=0)}=\frac{\int_{r=r_1}^{r=r_c} C(r,t)A(r)dr}{C_0\int_{r=r_1}^{r=r_c} A(r)dr} \tag{17}$$

where $A(r)$ is the cross-section area of the centrifuge tube used for performing the PUM experiments. For a given set of centrifugation condition (rotor type, rotation speed and the centrifuge tube geometry), the sedimentation function is uniquely determined by the distributed sedimentation and diffusion coefficients and, therefore, the distributed lengths and diameters of SWCNT particles in a given dispersion. The experimental protocols for measuring the sedimentation function of SWCNT dispersions as well as its theoretical derivation can be found in Liu et al 's work (Liu et al., 2008).

With the analytical solution of Eq. (15) for the concentration profile $C(r, t)$, the experimentally determined sedimentation function can be fitted by Eq. (17) to give the bulk averaged s and D values of a given SWCNT dispersion. It should be noted that, in comparison to the DLS technique, the PUM method intends to have an overestimation of the translational diffusion coefficient D. Therefore, to determine the structural information of SWCNTs by the PUM method with Eq. (4c) and Eq. (16), one has to separately measure the diffusion coefficient of the SWCNTs, e.g., by the DLS measurement. The PUM method has been successfully used for studying the processing-structure relationship of SWCNT

dispersions processed by sonication and microfluidization techniques (Luo et al., 2010). The comparative studies indicate that, in addition to the energy dissipation rate, the details of the flow field can play a critical role in dispersing and separating the SWCNT bundles into individual tubes.

To examine the PUM method against the commonly used AFM approach for characterizing the SWCNT structures, an individual-tube enriched SWCNT dispersion was prepared. In brief, an SWCNT/SDBS/H_2O dispersion was probe-sonicated for 30 minutes and then subject to ultracentrifugation for ~ 3hrs at 200, 000g. The supernatant, which is concentrated by individual tubes, was collected and examined by both the PUM and the AFM technique for determining the averaged length and diameter of the SWCNT particles. The PUM method was carried out with a fix-angle rotor by the Optima™ MAX-XP ultracentrifuge instrument (Beckman Coulter, Inc.) and the DLS measurement was performed with the Delsa Nano C Particle Size Analyzer (Beckman Coulter, Inc.). The experimentally determined and theoretically fitted sedimentation functions for both the as-sonicated and the individual tube enriched SWCNT dispersions are shown in Fig. 3a. The fitted values of the sedimentation coefficient, *s*, are given in Table 1. In the same table, the diffusion coefficients measured by the polarized DLS method, the bulk averaged length and diameter values calculated with Eq. (4c) and Eq. (16) are also listed. With a spin-coating based sample preparation protocol, the individual tube enriched SWCNT dispersion was also examined by the AFM technique. The representative topography image and the SWCNT length and diameter obtained by AFM are respectively shown in Fig. 3b and listed in Table 1. A reasonable agreement between the AFM measurement and the PUM method has been found for both the length and diameter of the examined individual SWCNTs.

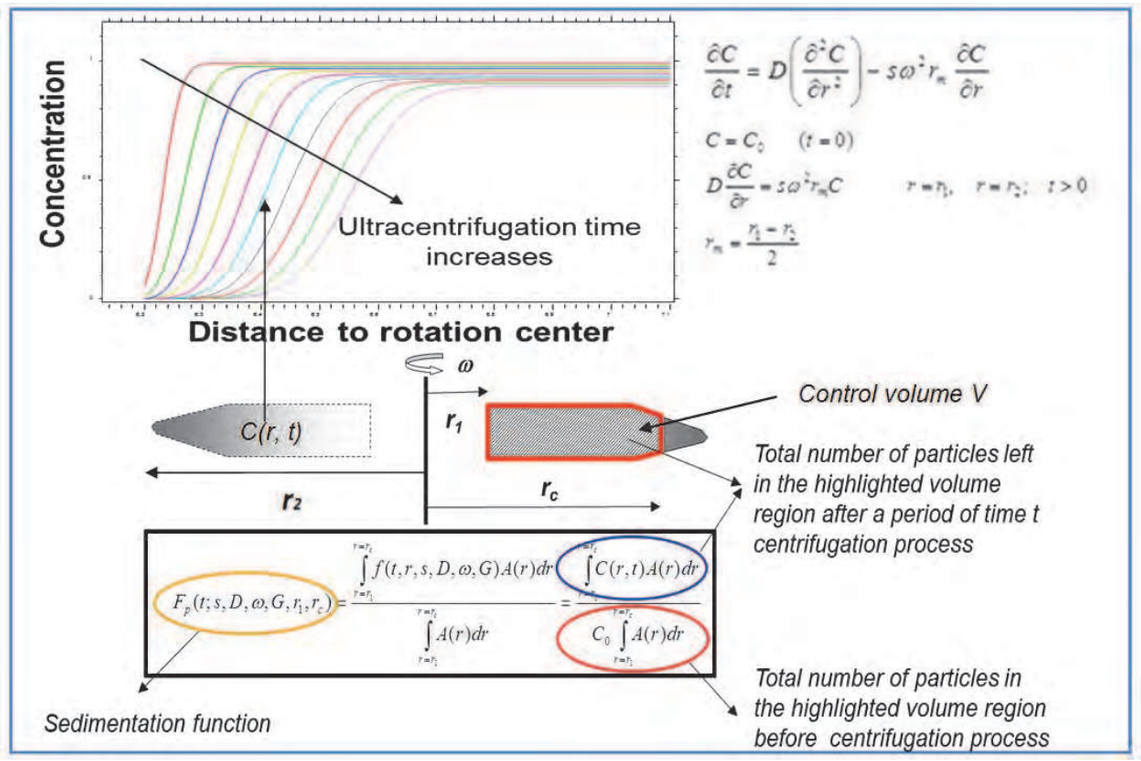

Fig. 2. Operational principle of analytical and preparative ultracentrifuge method for the structural characterization of SWCNT dispersions.

To further validate the PUM method, the sedimentation function for a standard polystyrene (PS) sphere dispersion in water (PS diameter of 100 nm) was determined experimentally and fitted theoretically, and the results are shown in Fig. 3c. Two different types of rotors, fixed-angle and swing-bucket, were used for comparing the effect of rotor geometry. With the sedimentation coefficient determined by the PUM method, the diameter of the PS sphere was accordingly calculated by:

$$d_{ps} = 2\sqrt{\frac{9s\eta_0}{2(\rho_{ps} - \rho_0)}} \tag{18}$$

The results are given in Table 1. The PUM determined PS sphere diameter deviates from the standard value of 100 nm by about 10%. Depending upon whether the fixed-angle rotor or the swing-bucket rotor is used, the PS diameter determined by the PUM method is 89.7 nm and 106.2 nm respectively. The effect of rotor geometry for the PUM method is clear.

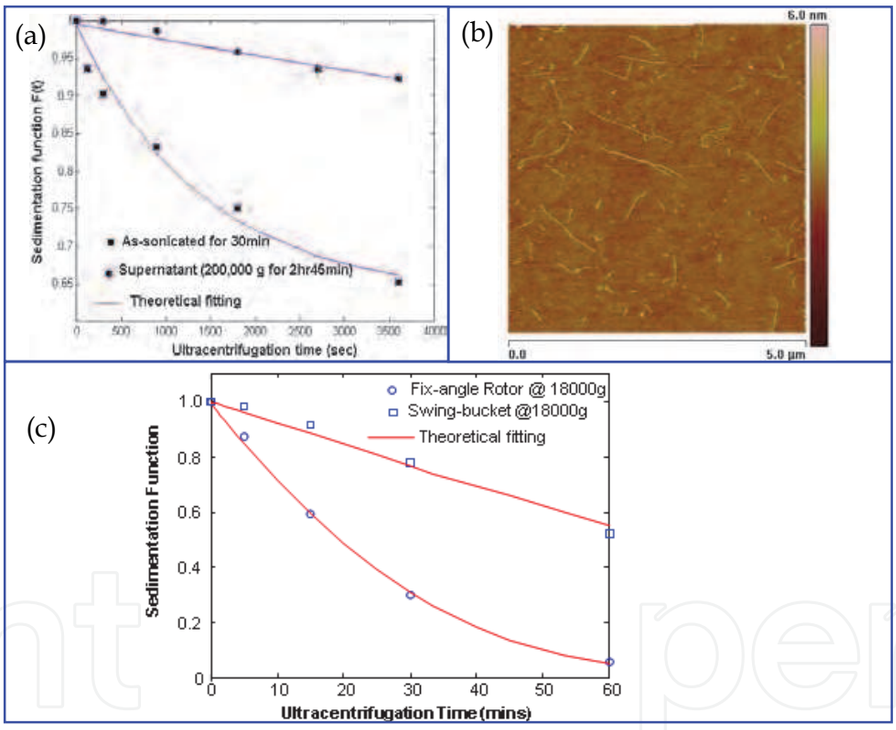

Fig. 3. (a) Experimentally determined and theoretically fitted sedimentation functions for as-sonicated and individual tube enriched SWCNT dispersions; Ultracentrifugation conditions – Fixed-angle rotor, 13,000 g for the as-sonicated dispersion and 65,000 g for the individual tube enriched dispersion; (b) AFM micrograph of the individual tube enriched SWCNT samples. Sample was prepared by spin coating and drying in the air on silicon wafer. (c) Experimentally determined and theoretically fitted sedimentation functions for the standard 100 nm PS sphere dispersion; Ultracentrifugation conditions – Fixed-angle rotor and Swing-bucket, 18, 000 g

Unlike the classical analytical ultracentrifuge approach, in which the concentration profile of the dispersion particles is mapped in the centrifugation process, the PUM method relies on a

post-centrifugation process to experimentally determine the sedimentation function. From the instrument perspective, this is a big advantage since there is no complicated real-time detection optics is involved for the PUM method.

SWCNT/SDBS/H_2O Dispersions				
AFM	PUM			
200,000 g Centrifuged	As-sonicated		200,000 g Centrifuged	
L = 603 ± 336 nm	s = 1.76×10^{-11} sec	L = 2541 nm	s = 2.40×10^{-13} sec	L = 821 nm
d=0.94 ± 0.28 nm	D = 1.12×10^{-8} cm^2/sec	d = 7.6 nm	D = 4.37×10^{-8} cm^2/sec	d = 0.82 nm
Standard 100 nm polystyrene spheres				
Standard	PUM			
100 nm	Fixed-angle rotor		Swing-bucket rotor	
	s = 2.46×10^{-11} sec	d = 89.7 nm	s = 3.45×10^{-11} sec	d = 106.2 nm

Table 1. Comparison of AFM and PUM method for characterizing the SWCNT structures and standard 100 nm PS spheres

5. Spectroscopic techniques for charactering the bundling states of SWCNTs

In an as-prepared and well-dispersed SWCNT dispersion, the SWCNTs may either exist as individual tubes or present in a SWNT bundle. The techniques introduced above, including the viscosity and rheological measurements, different scattering techniques, and the sedimentation characterization methods, can hardly provide a reliable estimation on the relative percentage of individual tubes or the exfoliation efficiency of SWCNT bundles in a given dispersion. Given the important roles of bundling states in studying the fundamental photophysics of SWCNT (O'Connell et al., 2002; Torrens et al., 2006; Tan et al., 2007; Tan et al., 2008) and developing high-performance SWCNT-reinforced nanocomposites (Liu & Kumar, 2003; Ajayan & Tour, 2007), it is critical to have the capability for quantitative characterization of the degree of exfoliation for a given SWCNT dispersion.

By observing the broadening and red-shift of the featured absorption peaks of SWCNTs (Hagen & Hertel, 2003), the UV-visible-NIR spectroscopy has been used for qualitatively distinguishing the individual tube enriched SWCNT dispersions from the bundled ones. Moreover, Raman spectroscopy was also intensively used for characterizing the spectral characteristics induced by SWCNT bundling, which includes, e.g., the frequency upshift of the radial breathing mode (RBM) (O'Connell et al., 2004; Izard et al., 2005) and G-band broadening (Cardenas, 2008; Husanu et al., 2008). Using a 785 nm laser as the excitation source, Heller et al. (Heller et al., 2004) demonstrated a positive correlation between the intensity of the 267 cm^{-1} RBM band and the bundling/aggregation states of various SWCNT samples. This valuable observation has been widely used for qualitative determination of the bundling states of SWCNT samples (Graupner, 2007; Kumatani & Warburton, 2008). The authors recently developed a simultaneous Raman scattering and PL spectroscopy technique (SRSPL) (Liu et al., 2009; Luo et al., 2010) to provide a new way for quantitative characterization of the bundling states of SWCNT dispersions.

When a laser interacts with a semi-conductive SWCNT, it can excite both the vibrational and electronic energy transition (Fig. 4a). As a result, one can detect the Raman scattered and the

PL emitted photons to acquire the Raman scattering and photoluminescence spectra (Burghard, 2005; Dresselhaus et al., 2005; Dresselhaus et al., 2007), from which the molecular/atomic and electronic structures of SWCNTs can be inferred.

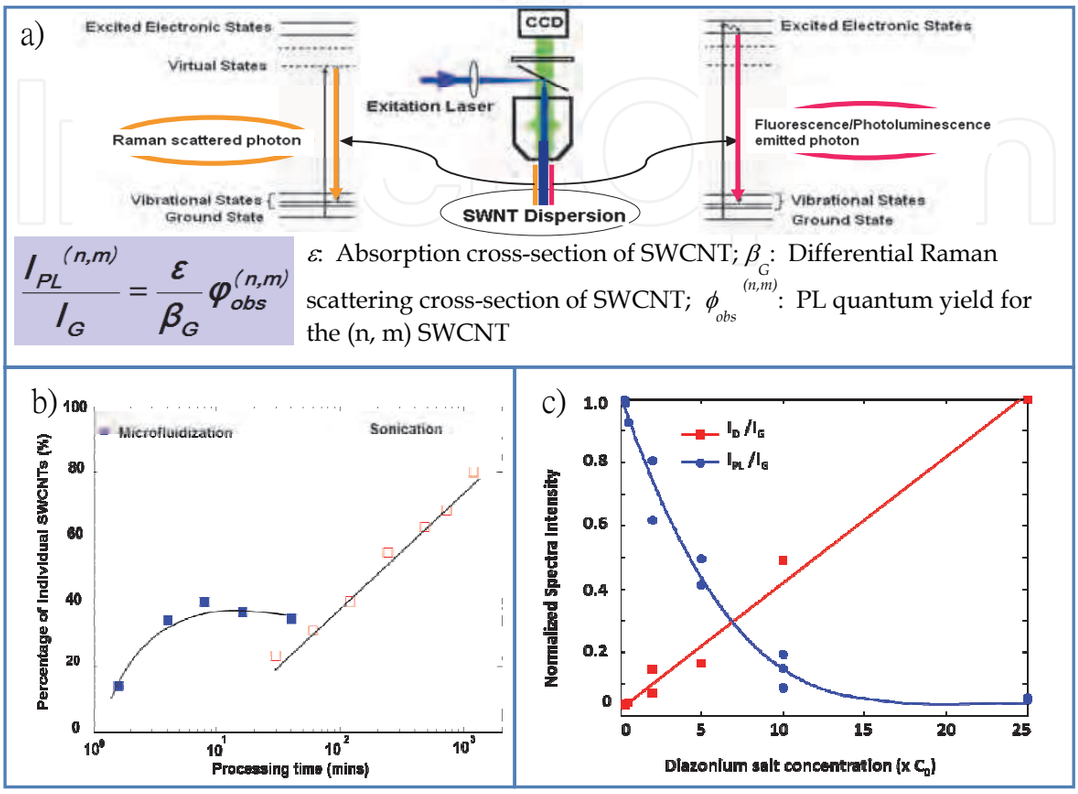

Fig. 4. Simultaneous Raman scattering and photoluminescence spectroscopy (SRSPL) for the degree of exfoliation and the defect density characterization of SWCNTs. a) operation principle of SRSPL method; b) SRSPL determined degree of exfoliation of SWCNTs processed by microfluidization and sonication; c) defect density characterization by SRSPL and Raman D-band for SWCNTs functionalized with diazonium salt.

In general, the Raman and PL spectra are taken separately by two different instruments – Raman spectrometer and fluorometer and analyzed independently. Nevertheless, as demonstrated in Liu et al's work (Liu et al., 2009), there is a significant advantage for acquiring the Raman and PL spectra of SWCNT dispersions simultaneously with the same optics. In this case, without introducing the complicated instrument correction factors, the intensity ratio of a PL band (I_{PL}) to a Raman band (I_{Raman}) is directly related to the intrinsic optical and spectroscopic properties of SWCNTs by:

$$\frac{I_{PL}}{I_{Raman}} = \frac{\varepsilon}{\beta}\Phi \tag{19}$$

where ε is the optical absorption cross-section, β is the Raman scattering cross-section, and Φ is the PL quantum yield of the SWCNT. Due to the presence of metallic SWCNTs in its very near neighbor, the PL of a semi-conductive SWCNT can be quenched when it is in a

SWCNT bundle. Using this fact and on the basis of Eq. (19), one can quantitatively determine the percentage of individual tubes or the degree of exfoliation for a given SWCNT dispersion with the SRSPL method (Liu et al., 2009; Luo et al., 2010). Fig. 4b compares the efficiency of the microfluidization and the sonication processes in exfoliating SWCNT bundles as examined by the SRSPL method. Again, it is clear that, the details of the flow field can play a critical role in separating the SWCNT bundles into individual tubes.

In addition to its capability for quantifying the degree of exfoliation, the SRSPL can also be used for characterizing the defect density of chemically functionalized SWCNTs. This is based on that, upon chemical functionalization, the defects introduced on the sidewall of a semi-conductive SWCNT effectively reduced the defect-free segment length, which cause a reduced PL quantum yield (Rajan et al., 2008). Fig. 4c demonstrated the SRSPL method for characterizing the defect density of diazonium salt functionalized SWCNTs (Xiao et al., 2010). In the same figure, the commonly used Raman D-band over G-band ratio (Graupner, 2007) for the same purpose is also shown for comparison. It is clear that the SRSPL and the Raman D-band method complement to each other; the former is suitable for low defect density and the latter is more appropriate for high defect density characterization.

6. Conclusion

The hierarchical structures of SWCNTs with a broad range length scales can be found in a dispersion, which may include: 1) individual tubes with different molecular structure as specified by the rolling or chiral vector (n, m); 2) SWCNT bundles that is composed of multiple individual tubes approximately organized into a 2D hexagonal lattice with their long axis parallel to each other; 3) SWCNT aggregates formed by the topological entanglement or enmeshment of individual tubes and/or SWCNT bundles; 4) SWCNT network that spans the overall dispersion sample. In order to establish the processing-structure-property relationship of SWCNT enabled multifunction nanocomposites and SWCNT dispersion related novel applications, an in-situ and quantitative characterization of the hierarchical structures of SWCNTs in the dispersion is necessary. With an emphasis on the underlying physical principles, the recently emerging experimental techniques that enable an in-situ and quantitative structural characterization of SWCNT dispersions are reviewed in this chapter, which include: 1) *Viscosity and rheological measurements; 2) Elastic and quasi-elastic scattering techniques; 3) Sedimentation characterization methods; and 4) Spectroscopic techniques*. Each of these techniques has its own length-scale vantage for the structural characterization of SWCNTs in the dispersion. To fully characterize the hierarchical structures of SWCNTs in the dispersion and understand their roles in controlling the properties and performance of SWCNT enabled multifunction nanocomposites and SWCNT dispersion related novel applications, the best approach is to be able to wisely and coherently utilize the introduced techniques to their advantages. For different reasons, the hierarchical structures of SWCNTs in the dispersion are subject to a certain distribution. This brings out the polydispersity issues, which have not been addressed by the experimental techniques being reviewed here. Future research should be directed toward overcoming this even more challenging issue.

7. Reference

Ajayan, P. M. & Tour, J. M. (2007). Materials science - Nanotube composites. *Nature*, Vol. 447, No. 7148, pp. 1066-1068, ISSN 0028-0836

Avalos, J. B.; Rubi, J. M. & Bedeaux, D. (1993). Dynamics of rodlike polymers in dilute solution. *Macromolecules*, Vol. 26, No. 10, pp. 2550-2561, ISSN 0024-9297

Avouris, P.; Freitag, M. & Perebeinos, V. (2008). Carbon-nanotube optoelectronics, In: *Carbon Nanotubes*, pp. 423-454, Springer-Verlag Berlin, ISBN 0303-4216, Berlin, Germany

Azoubel, S. & Magdassi, S. (2010). The formation of carbon nanotube dispersions by high pressure homogenization and their rapid characterization by analytical centrifuge. *Carbon*, Vol. 48, No. 12, pp. 3346-3352, ISSN 0008-6223

Badaire, S.; Poulin, P.; Maugey, M. & Zakri, C. (2004). In situ measurements of nanotube dimensions in suspensions by depolarized dynamic light scattering. *Langmuir*, Vol. 20, No. 24, pp. 10367-10370, ISSN 0743-7463

Ballauff, M.; Bolze, J.; Dingenouts, N.; Hickl, P. & Potschke, D. (1996). Small-angle X-ray scattering on latexes. *Macromolecular Chemistry and Physics*, Vol. 197, No. 10, pp. 359-377

Batchelor, G. K. (1974). Transport properties of two-phase materials with random structure. *Annual Review of Fluid Mechanics*, Vol. 6, pp. 227-255, ISSN 0066-4189

Bauer, B. J.; Hobbie, E. K. & Becker, M. L. (2006). Small-angle neutron scattering from labeled single-wall carbon nanotubes. *Macromolecules*, Vol. 39, No. 7, pp. 2637-2642, ISSN 0024-9297

Baughman, R. H.; Zakhidov, A. A. & de Heer, W. A. (2002). Carbon nanotubes - the route toward applications. *Science*, Vol. 297, No. 5582, pp. 787-792, ISSN 0036-8075

Bergin, S. D.; Nicolosi, V.; Giordani, S.; de Gromard, A.; Carpenter, L.; Blau, W. J. & Coleman, J. N. (2007). Exfoliation in ecstasy: liquid crystal formation and concentration-dependent debundling observed for single-wall nanotubes dispersed in the liquid drug gamma-butyrolactone. *Nanotechnology*, Vol. 18, No. 45, pp. 10, ISSN 0957-4484

Berne, B. J. & Pecora, R. (2000). *Dynamic Light Scattering with Applications to Chemistry, Biology, and Physics* Dover Publications, Inc., ISBN 978-0486411552, New York, USA

Bicerano, J.; Douglas, J. F. & Brune, D. A. (1999). Model for the viscosity of particle dispersions. *Journal of Macromolecular Science-Reviews in Macromolecular Chemistry and Physics*, Vol. C39, No. 4, pp. 561-642, ISSN 0736-6574

Bonard, J. M.; Salvetat, J. P.; Stockli, T.; de Heer, W. A.; Forro, L. & Chatelain, A. (1998). Field emission from single-wall carbon nanotube films. *Applied Physics Letters*, Vol. 73, No. 7, pp. 918-920, ISSN 0003-6951

Brown, P. H. & Schuck, P. (2006). Macromolecular size-and-shape distributions by sedimentation velocity analytical ultracentrifugation. *Biophysical Journal*, Vol. 90, No. 12, pp. 4651-4661, ISSN 0006-3495

Burghard, M. (2005). Electronic and vibrational properties of chemically modified single-wall carbon nanotubes. *Surface Science Reports*, Vol. 58, No. 1-4, pp. 1-109, ISSN 0167-5729

Cao, J.; Wang, Q. & Dai, H. J. (2003). Electromechanical properties of metallic, quasimetallic, and semiconducting carbon nanotubes under stretching. *Physical Review Letters*, Vol. 90, No. 15, pp. 4, ISSN 0031-9007

Cao, Q. & Rogers, J. A. (2009). Ultrathin Films of Single-Walled Carbon Nanotubes for Electronics and Sensors: A Review of Fundamental and Applied Aspects. *Advanced Materials*, Vol. 21, No. 1, pp. 29-53, ISSN 0935-9648

Cardenas, J. F. (2008). Protonation and sonication effects on aggregation sensitive Raman features of single wall carbon nanotubes. *Carbon*, Vol. 46, No. 10, pp. 1327-1330, ISSN 0008-6223

Chen, Q.; Saltiel, C.; Manickavasagam, S.; Schadler, L. S.; Siegel, R. W. & Yang, H. C. (2004). Aggregation behavior of single-walled carbon nanotubes in dilute aqueous suspension. *Journal of Colloid and Interface Science*, Vol. 280, No. 1, pp. 91-97, ISSN 0021-9797

Chou, T. W.; Gao, L. M.; Thostenson, E. T.; Zhang, Z. G. & Byun, J. H. (2010). An assessment of the science and technology of carbon nanotube-based fibers and composites. *Composites Science and Technology*, Vol. 70, No. 1, pp. 1-19, ISSN 0266-3538

Chu, B. (1991). *Laser light scattering: basic principles and practice* (2nd), Academic Press, ISBN 9780486457987 Boston, USA

Colfen, H. & Volkel, A. (2004). Analytical ultracentrifugation in colloid chemistry, In: *Analytical Ultracentrifugation Vii*, Lechner, M. D. and Borger, L., pp. 31-47, Springer-Verlag Berlin, Berlin, Germany

Cotiuga, I.; Picchioni, F.; Agarwal, U. S.; Wouters, D.; Loos, J. & Lemstra, P. J. (2006). Block-copolymer-assisted solubilization of carbon nanotubes and exfoliation monitoring through viscosity. *Macromolecular Rapid Communications*, Vol. 27, No. 13, pp. 1073-1078, ISSN 1022-1336

Davis, V. A.; Ericson, L. M.; Parra-Vasquez, A. N. G.; Fan, H.; Wang, Y. H.; Prieto, V.; Longoria, J. A.; Ramesh, S.; Saini, R. K.; Kittrell, C.; Billups, W. E.; Adams, W. W.; Hauge, R. H.; Smalley, R. E. & Pasquali, M. (2004). Phase Behavior and rheology of SWNTs in superacids. *Macromolecules*, Vol. 37, No. 1, pp. 154-160, ISSN 0024-9297

Dresselhaus, M. S.; Dresselhaus, G.; Saito, R. & Jorio, A. (2005). Raman spectroscopy of carbon nanotubes. *Physics Reports-Review Section of Physics Letters*, Vol. 409, No. 2, pp. 47-99, ISSN 0370-1573

Dresselhaus, M. S.; Dresselhaus, G.; Saito, R. & Jorio, A. (2007). Exciton photophysics of carbon nanotubes. *Annual Review of Physical Chemistry*, Vol. 58, pp. 719-747, ISSN 0066-426X

Dror, Y.; Pyckhout-Hintzen, W. & Cohen, Y. (2005). Conformation of polymers dispersing single-walled carbon nanotubes in water: A small-angle neutron scattering study. *Macromolecules*, Vol. 38, No. 18, pp. 7828-7836, ISSN 0024-9297

Duggal, R. & Pasquali, M. (2006). Dynamics of individual single-walled carbon nanotubes in water by real-time visualization. *Physical Review Letters*, Vol. 96, No. 24, pp. 4, ISSN 0031-9007

Fakhri, N.; Tsyboulski, D. A.; Cognet, L.; Weisman, R. B. & Pasquali, M. (2009). Diameter-dependent bending dynamics of single-walled carbon nanotubes in liquids. *Proceedings of the National Academy of Sciences of the United States of America*, Vol. 106, No. 34, pp. 14219-14223, ISSN 0027-8424

Feigin, L. A. & Svergun, D. I. (1987). *Structure Analysis by Small-Angle X-ray and Neutron Scattering* Plenum Press, ISBN 978-0306426292, New York, USA

Flory, P. J. (1978). Statistical thermodynamics of mixtures of rodlike particles. 5. Mixtures with random coils. *Macromolecules*, Vol. 11, No. 6, pp. 1138-1141, ISSN 0024-9297

Fujita, H. (1975). *Foundations of Ultracentrifugal Analysis* John Wiley & Sons, ISBN 9780471285823, New York, USA

Giordani, S.; Bergin, S.; Nicolosi, V.; Lebedkin, S.; Blau, W. J. & Coleman, J. N. (2006). Fabrication of stable dispersions containing up to 70% individual carbon nanotubes in a common organic solvent. *Physica Status Solidi B-Basic Solid State Physics*, Vol. 243, No. 13, pp. 3058-3062, ISSN 0370-1972

Girifalco, L. A.; Hodak, M. & Lee, R. S. (2000). Carbon nanotubes, buckyballs, ropes, and a universal graphitic potential. *Physical Review B*, Vol. 62, No. 19, pp. 13104-13110, ISSN 0163-1829

Glatter, O. & Kratky, O. (1982). *Small Angle X-ray Scattering* Academic Press, ISBN 978-0122862809, London, UK

Grady, B. P. (2009). Recent Developments Concerning the Dispersion of Carbon Nanotubes in Polymers. *Macromolecular Rapid Communications*, Vol. 31, No. 3, pp. 247-257, ISSN 1022-1336

Graessley, W. W. (2004). *Polymeric Liquids and Networks: Structure and Properties* Garland Science, ISBN 978-0-8153-4169-7, New York and London

Granite, M.; Radulescu, A.; Pyckhout-Hintzen, W. & Cohen, Y. (2010). Interactions between Block Copolymers and Single-Walled Carbon Nanotubes in Aqueous Solutions: A Small-Angle Neutron Scattering Study. *Langmuir*, Vol. 27, No. 2, pp. 751-759, ISSN 0743-7463

Graupner, R. (2007). Raman spectroscopy of covalently functionalized single-wall carbon nanotubes. *Journal of Raman Spectroscopy*, Vol. 38, No. 6, pp. 673-683, ISSN 0377-0486

Green, M. J.; Behabtu, N.; Pasquali, M. & Adams, W. W. (2009). Nanotubes as polymers. *Polymer*, Vol. 50, No. 21, pp. 4979-4997, ISSN 0032-3861

Grow, R. J.; Wang, Q.; Cao, J.; Wang, D. W. & Dai, H. J. (2005). Piezoresistance of carbon nanotubes on deformable thin-film membranes. *Applied Physics Letters*, Vol. 86, No. 9, pp. 3, ISSN 0003-6951

Gruner, G. (2006). Carbon nanotube films for transparent and plastic electronics. *Journal of Materials Chemistry*, Vol. 16, No. 35, pp. 3533-3539, ISSN 0959-9428

Guinier, A. & Fournet, G. (1955). *Small-Angle Scattering of X-rays* (1st), Wiley, New York, USA

Hagen, A. & Hertel, T. (2003). Quantitative analysis of optical spectra from individual single-wall carbon nanotubes. *Nano Letters*, Vol. 3, No. 3, pp. 383-388, ISSN 1530-6984

Heller, D. A.; Barone, P. W.; Swanson, J. P.; Mayrhofer, R. M. & Strano, M. S. (2004). Using Raman spectroscopy to elucidate the aggregation state of single-walled carbon nanotubes. *Journal of Physical Chemistry B*, Vol. 108, No. 22, pp. 6905-6909, ISSN 1520-6106

Higgins, J. S. & Benoit, H. C. (1994). *Polymers and Neutron Scattering* Oxford University Press, ISBN 978-0-19-850063-6, New York, USA

Hilding, J.; Grulke, E. A.; Zhang, Z. G. & Lockwood, F. (2003). Dispersion of carbon nanotubes in liquids. *Journal of Dispersion Science and Technology*, Vol. 24, No. 1, pp. 1-41, ISSN 0193-2691

Hornsby, P. R. (1999). Rheology, compounding and processing of filled thermoplastics, In: *Mineral Fillers in Thermoplastics I*, pp. 155-217, Springer-Verlag Berlin, ISBN 0065-3195, Berlin, Germany

Hough, L. A.; Islam, M. F.; Hammouda, B.; Yodh, A. G. & Heiney, P. A. (2006). Structure of semidilute single-wall carbon nanotube suspensions and gels. *Nano Letters*, Vol. 6, No. 2, pp. 313-317, ISSN 1530-6984

Hough, L. A.; Islam, M. F.; Janmey, P. A. & Yodh, A. G. (2004). Viscoelasticity of single wall carbon nanotube suspensions. *Physical Review Letters*, Vol. 93, No. 16, pp. 4, ISSN 0031-9007

Husanu, M.; Baibarac, M. & Baltog, I. (2008). Non-covalent functionalization of carbon nanotubes: Experimental evidence for isolated and bundled tubes. *Physica E-Low-Dimensional Systems & Nanostructures*, Vol. 41, No. 1, pp. 66-69, ISSN 1386-9477

Hussain, F.; Hojjati, M.; Okamoto, M. & Gorga, R. E. (2006). Review article: Polymer-matrix nanocomposites, processing, manufacturing, and application: An overview. *Journal of Composite Materials*, Vol. 40, No. 17, pp. 1511-1575, ISSN 0021-9983

Islam, M. F.; Rojas, E.; Bergey, D. M.; Johnson, A. T. & Yodh, A. G. (2003). High weight fraction surfactant solubilization of single-wall carbon nanotubes in water. *Nano Letters*, Vol. 3, No. 2, pp. 269-273, ISSN 1530-6984

Izard, N.; Riehl, D. & Anglaret, E. (2005). Exfoliation of single-wall carbon nanotubes in aqueous surfactant suspensions: A Raman study. *Physical Review B*, Vol. 71, No. 19, pp. 7, ISSN 1098-0121

Jeffrey, D. J. & Acrivos, A. (1976). The rheological properties of suspensions of rigid particles. *Aiche Journal*, Vol. 22, No. 3, pp. 417-432, ISSN 0001-1541

Kayatin, M. J. & Davis, V. A. (2009). Viscoelasticity and Shear Stability of Single-Walled Carbon Nanotube/Unsaturated Polyester Resin Dispersions. *Macromolecules*, Vol. 42, No. 17, pp. 6624-6632, ISSN 0024-9297

Kumatani, A. & Warburton, P. A. (2008). Characterization of the disaggregation state of single-walled carbon nanotube bundles by dielectrophoresis and Raman spectroscopy. *Applied Physics Letters*, Vol. 92, No. 24, pp. 3, ISSN 0003-6951

Larson, R. G. (1999). *The Structure and Rheology of Complex Fluids* Oxford University Press, ISBN 978-019-5121-97-1, New York, USA

Laue, T. M. & Stafford, W. F. (1999). Modern applications of analytical ultracentrifugation. *Annual Review of Biophysics and Biomolecular Structure*, Vol. 28, pp. 75-100, ISSN 1056-8700

Lehner, D.; Lindner, H. & Glatter, O. (2000). Determination of the translational and rotational diffusion coefficients of rodlike particles using depolarized dynamic light scattering. *Langmuir*, Vol. 16, No. 4, pp. 1689-1695, ISSN 0743-7463

Li, Z. L.; Dharap, P.; Nagarajaiah, S.; Barrera, E. V. & Kim, J. D. (2004). Carbon nanotube film sensors. *Advanced Materials*, Vol. 16, No. 7, pp. 640-+, ISSN 0935-9648

Liu, T. & Kumar, S. (2003). Effect of orientation on the modulus of SWNT films and fibers. *Nano Letters*, Vol. 3, No. 5, pp. 647-650, ISSN 1530-6984

Liu, T.; Luo, S. D.; Xiao, Z. W.; Zhang, C. & Wang, B. (2008). Preparative Ultracentrifuge Method for Characterization of Carbon Nanotube Dispersions. *Journal of Physical Chemistry C*, Vol. 112, No. 49, pp. 19193-19202, ISSN 1932-7447

Liu, T.; Xiao, Z. W. & Wang, B. (2009). The exfoliation of SWCNT bundles examined by simultaneous Raman scattering and photoluminescence spectroscopy. *Carbon*, Vol. 47, No. 15, pp. 3529-3537, ISSN 0008-6223

Liu, Y. Q.; Gao, L.; Zheng, S.; Wang, Y.; Sun, J.; Kajiura, H.; Li, Y. & Noda, K. (2007). Debundling of single-walled carbon nanotubes by using natural polyelectrolytes. *Nanotechnology*, Vol. 18, No. 36, pp. 6, ISSN 0957-4484

Luo, S. D.; Liu, T. & Wang, B. (2010). Comparison of ultrasonication and microfluidization for high throughput and large-scale processing of SWCNT dispersions. *Carbon*, Vol. 48, No. 10, pp. 2992-2994, ISSN 0008-6223

Ma, A. W. K.; Chinesta, F. & Mackley, M. R. (2009). The rheology and modeling of chemically treated carbon nanotubes suspensions. *Journal of Rheology*, Vol. 53, No. 3, pp. 547-573, ISSN 0148-6055

Mac Kernan, D. & Blau, W. J. (2008). Exploring the mechanisms of carbon-nanotube dispersion aggregation in a highly polar solvent. *Epl*, Vol. 83, No. 6, pp. 6, ISSN 0295-5075

Mansfield, M. L. & Douglas, J. F. (2008). Transport properties of rodlike particles. *Macromolecules*, Vol. 41, No. 14, pp. 5422-5432, ISSN 0024-9297

Mason, M. & Weaver, W. (1926). The settling of small particles in a fluid. *Physical Review*, Vol. 23, pp. 412-426

Metzner, A. B. (1985). Rheology of suspensions in polymeric liquids. *Journal of Rheology*, Vol. 29, No. 6, pp. 739-775, ISSN 0148-6055

Moniruzzaman, M. & Winey, K. I. (2006). Polymer nanocomposites containing carbon nanotubes. *Macromolecules*, Vol. 39, No. 16, pp. 5194-5205, ISSN 0024-9297

Moore, V. C.; Strano, M. S.; Haroz, E. H.; Hauge, R. H.; Smalley, R. E.; Schmidt, J. & Talmon, Y. (2003). Individually suspended single-walled carbon nanotubes in various surfactants. *Nano Letters*, Vol. 3, No. 10, pp. 1379-1382, ISSN 1530-6984

O'Connell, M. J.; Bachilo, S. M.; Huffman, C. B.; Moore, V. C.; Strano, M. S.; Haroz, E. H.; Rialon, K. L.; Boul, P. J.; Noon, W. H.; Kittrell, C.; Ma, J. P.; Hauge, R. H.; Weisman, R. B. & Smalley, R. E. (2002). Band gap fluorescence from individual single-walled carbon nanotubes. *Science*, Vol. 297, No. 5581, pp. 593-596, ISSN 0036-8075

O'Connell, M. J.; Sivaram, S. & Doorn, S. K. (2004). Near-infrared resonance Raman excitation profile studies of single-walled carbon nanotube intertube interactions: A direct comparison of bundled and individually dispersed HiPco nanotubes. *Physical Review B*, Vol. 69, No. 23, pp. 15, ISSN 1098-0121

Oh, C. & Sorensen, C. M. (1999). Scaling approach for the structure factor of a generalized system of scatterers. *Journal of Nanoparticle Research*, Vol. 1, pp. 369-377.

Onsager, L. (1949). The effects of shape on the interaction of colloidal particles. *Annals of the New York Academy of Sciences*, Vol. 51, No. 4, pp. 627-659, ISSN 0077-8923

Parra-Vasquez, A. N. G.; Stepanek, I.; Davis, V. A.; Moore, V. C.; Haroz, E. H.; Shaver, J.; Hauge, R. H.; Smalley, R. E. & Pasquali, M. (2007). Simple length determination of single-walled carbon nanotubes by viscosity measurements in dilute suspensions. *Macromolecules*, Vol. 40, No. 11, pp. 4043-4047, ISSN 0024-9297

Pedersen, J. S. (1997). Analysis of small-angle scattering data from colloids and polymer solutions: modeling and least-squares fitting. *Advances in Colloid and Interface Science*, Vol. 70, pp. 171-210, ISSN 0001-8686

Peterlik, H. & Fratzl, P. (2006). Small-angle X-ray scattering to characterize nanostructures in inorganic and hybrid materials chemistry. *Monatshefte Fur Chemie*, Vol. 137, No. 5, pp. 529-543, ISSN 0026-9247

Petrie, C. J. S. (1999). The rheology of fibre suspensions. *Journal of Non-Newtonian Fluid Mechanics*, Vol. 87, No. 2-3, pp. 369-402, ISSN 0377-0257

Pollet, R. J.; Haase, B. A. & Standaert, M. L. (1979). Macromolecular characterization by sedimentation equilibrium in the preparative ultra-centrifuge. *Journal of Biological Chemistry*, Vol. 254, No. 1, pp. 30-33, ISSN 0021-9258

Rajan, A.; Strano, M. S.; Heller, D. A.; Hertel, T. & Schulten, K. (2008). Length-dependent optical effects in single walled carbon nanotubes. *Journal of Physical Chemistry B*, Vol. 112, No. 19, pp. 6211-6213, ISSN 1520-6106

Russel, W. B. (1980). Review of the role of colloidal forces in the rheology of suspensions. *Journal of Rheology*, Vol. 24, No. 3, pp. 287-317, ISSN 0148-6055

Sahoo, N. G.; Rana, S.; Cho, J. W.; Li, L. & Chan, S. H. (2010). Polymer nanocomposites based on functionalized carbon nanotubes. *Progress in Polymer Science*, Vol. 35, No. 7, pp. 837-867, ISSN 0079-6700

Saito, R.; Dresselhaus, G. & Dresselhaus, M. S. (1998). *Physical Properties of Carbon Nanotubes* Imperial College Press, ISBN 1-86094-223-7, London, UK

Salvetat, J. P.; Briggs, G. A. D.; Bonard, J. M.; Bacsa, R. R.; Kulik, A. J.; Stockli, T.; Burnham, N. A. & Forro, L. (1999). Elastic and shear moduli of single-walled carbon nanotube ropes. *Physical Review Letters*, Vol. 82, No. 5, pp. 944-947, ISSN 0031-9007

Schaefer, D.; Brown, J. M.; Anderson, D. P.; Zhao, J.; Chokalingam, K.; Tomlin, D. & Ilavsky, J. (2003). Structure and dispersion of carbon nanotubes. *Journal of Applied Crystallography*, Vol. 36, pp. 553-557, ISSN 0021-8898

Schaefer, D. W. & Justice, R. S. (2007). How nano are nanocomposites? *Macromolecules*, Vol. 40, No. 24, pp. 8501-8517, ISSN 0024-9297

Schaefer, D. W.; Zhao, J.; Brown, J. M.; Anderson, D. P. & Tomlin, D. W. (2003). Morphology of dispersed carbon single-walled nanotubes. *Chemical Physics Letters*, Vol. 375, No. 3-4, pp. 369-375, ISSN 0009-2614

Shenoy, A. V. (1999). *Rheology of filled polymer system* (1st), Springer, ISBN 978-041-2831-0-03, New York, USA

Shetty, A. M.; Wilkins, G. M. H.; Nanda, J. & Solomon, M. J. (2009). Multiangle Depolarized Dynamic Light Scattering of Short Functionalized Single-Walled Carbon Nanotubes. *Journal of Physical Chemistry C*, Vol. 113, No. 17, pp. 7129-7133, ISSN 1932-7447

Shiragami, N. & Kajiuchi, T. (1990). Precipitation of protein by ultracentrifuge with angle rotor. 1. Model for sedimentation process. *Bioprocess Engineering*, Vol. 5, No. 2, pp. 85-88, ISSN 0178-515X

Shiragami, N.; Kajiuchi, T. & Matsuda, A. (1990). Precipitation of protein by ultracentrifuge with angle rotor. 2. Experimental. *Bioprocess Engineering*, Vol. 5, No. 3, pp. 103-105, ISSN 0178-515X

Skakalova, V.; Kaiser, A. B.; Woo, Y. S. & Roth, S. (2006). Electronic transport in carbon nanotubes: From individual nanotubes to thin and thick networks. *Physical Review B*, Vol. 74, No. 8, pp. 10, ISSN 1098-0121

Snow, E. S.; Campbell, P. M.; Ancona, M. G. & Novak, J. P. (2005). High-mobility carbon-nanotube thin-film transistors on a polymeric substrate. *Applied Physics Letters*, Vol. 86, No. 3, pp. 3, ISSN 0003-6951

Sorensen, C. M. (2001). Light scattering by fractal aggregates: A review. *Aerosol Science and Technology*, Vol. 35, No. 2, pp. 648-687, ISSN 0278-6826

Tan, P. H.; Hasan, T.; Bonaccorso, F.; Scardaci, V.; Rozhin, A. G.; Milne, W. I. & Ferrari, A. C. (2008). Optical properties of nanotube bundles by photoluminescence excitation and absorption spectroscopy. *Physica E-Low-Dimensional Systems & Nanostructures*, Vol. 40, No. 7, pp. 2352-2359, ISSN 1386-9477

Tan, P. H.; Rozhin, A. G.; Hasan, T.; Hu, P.; Scardaci, V.; Milne, W. I. & Ferrari, A. C. (2007). Photoluminescence spectroscopy of carbon nanotube bundles: Evidence for exciton energy transfer. *Physical Review Letters*, Vol. 99, No. 13, pp. 4, ISSN 0031-9007

Teraoka, I. (2002). *Polymer Solutions: An Introduction to Physical Properties* John Wiley & Sons, Inc., ISBN 978-0471389293, New York, USA

Thess, A.; Lee, R.; Nikolaev, P.; Dai, H. J.; Petit, P.; Robert, J.; Xu, C. H.; Lee, Y. H.; Kim, S. G.; Rinzler, A. G.; Colbert, D. T.; Scuseria, G. E.; Tomanek, D.; Fischer, J. E. & Smalley, R. E. (1996). Crystalline ropes of metallic carbon nanotubes. *Science*, Vol. 273, No. 5274, pp. 483-487, ISSN 0036-8075

Torrens, O. N.; Milkie, D. E.; Zheng, M. & Kikkawa, J. M. (2006). Photoluminescence from intertube carrier migration in single-walled carbon nanotube bundles. *Nano Letters*, Vol. 6, No. 12, pp. 2864-2867, ISSN 1530-6984

Tracy, M. A. & Pecora, R. (1992). Dynamics of rigid and semirigid rodlike polymers. *Annual Review of Physical Chemistry*, Vol. 43, pp. 525-557, ISSN 0066-426X

Tummala, N. R. & Striolo, A. (2009). SDS Surfactants on Carbon Nanotubes: Aggregate Morphology. *Acs Nano*, Vol. 3, No. 3, pp. 595-602, ISSN 1936-0851

Urbina, A.; Miguel, C.; Delgado, J. L.; Langa, F.; Diaz-Paniagua, C. & Batallan, F. (2008). Isolated rigid rod behavior of functionalized single-wall carbon nanotubes in solution determined via small-angle neutron scattering. *Physical Review B*, Vol. 78, No. 4, pp. 5, ISSN 1098-0121

Vroege, G. J. & Lekkerkerker, H. N. W. (1992). Phase-transitions in lyotropic colloidal and polymer liquid-crystals. *Reports on Progress in Physics*, Vol. 55, No. 8, pp. 1241-1309, ISSN 0034-4885

Wang, H.; Christopherson, G. T.; Xu, Z. Y.; Porcar, L.; Ho, D. L.; Fry, D. & Hobbie, E. K. (2005). Shear-SANS study of single-walled carbon nanotube suspensions. *Chemical Physics Letters*, Vol. 416, No. 1-3, pp. 182-186, ISSN 0009-2614

Waugh, D. F. & Yphantis, D. A. (1953). Transient solute distributions from the basic equation of the ultracentrifuge. *Journal of Physical Chemistry*, Vol. 57, No. 3, pp. 312-318, ISSN 0022-3654

Xiao, Z. W.; Wang, B. & Liu, T. (2010). Simultaneous Raman scattering and photoluminescence spectroscopy for quantifying the chemically induced defects of single-walled carbon nanotubes, *Proceedings of American Society for Composites Twenty-Fifth Technical Conference*, Dayton, OH, USA, September 2010

Xu, Z. J.; Yang, X. N. & Yang, Z. (2010). A Molecular Simulation Probing of Structure and Interaction for Supramolecular Sodium Dodecyl Sulfate/Single-Wall Carbon Nanotube Assemblies. *Nano Letters*, Vol. 10, No. 3, pp. 985-991, ISSN 1530-6984

Yakobson, B. I. & Couchman, L. S. (2006). Persistence length and nanomechanics of random bundles of nanotubes. *Journal of Nanoparticle Research*, Vol. 8, No. 1, pp. 105-110, ISSN 1388-0764

Yamakawa, H. (1975). Viscoelastic properties of straight cylindrical macromolecules in dilute solution. *Macromolecules*, Vol. 8, No. 3, pp. 339-342, ISSN 0024-9297

Yurekli, K.; Mitchell, C. A. & Krishnamoorti, R. (2004). Small-angle neutron scattering from surfactant-assisted aqueous dispersions of carbon nanotubes. *Journal of the American Chemical Society*, Vol. 126, No. 32, pp. 9902-9903, ISSN 0002-7863

Zheng, M.; Jagota, A.; Semke, E. D.; Diner, B. A.; McLean, R. S.; Lustig, S. R.; Richardson, R. E. & Tassi, N. G. (2003). DNA-assisted dispersion and separation of carbon nanotubes. *Nature Materials*, Vol. 2, No. 5, pp. 338-342, ISSN 1476-1122

Zhou, W.; Islam, M. F.; Wang, H.; Ho, D. L.; Yodh, A. G.; Winey, K. I. & Fischer, J. E. (2004). Small angle neutron scattering from single-wall carbon nanotube suspensions: evidence for isolated rigid rods and rod networks. *Chemical Physics Letters*, Vol. 384, No. 1-3, pp. 185-189, ISSN 0009-2614

Carbon Nanotubes - Synthesis, Characterization, Applications

Edited by Dr. Siva Yellampalli

ISBN 978-953-307-497-9
Hard cover, 514 pages
Publisher InTech
Published online 20, July, 2011
Published in print edition July, 2011

Carbon nanotubes are one of the most intriguing new materials with extraordinary properties being discovered in the last decade. The unique structure of carbon nanotubes provides nanotubes with extraordinary mechanical and electrical properties. The outstanding properties that these materials possess have opened new interesting researches areas in nanoscience and nanotechnology. Although nanotubes are very promising in a wide variety of fields, application of individual nanotubes for large scale production has been limited. The main roadblocks, which hinder its use, are limited understanding of its synthesis and electrical properties which lead to difficulty in structure control, existence of impurities, and poor processability. This book makes an attempt to provide indepth study and analysis of various synthesis methods, processing techniques and characterization of carbon nanotubes that will lead to the increased applications of carbon nanotubes.

INTECH
open science | open minds

InTech Europe
University Campus STeP Ri
Slavka Krautzeka 83/A
51000 Rijeka, Croatia
Phone: +385 (51) 770 447
Fax: +385 (51) 686 166
www.intechopen.com

InTech China
Unit 405, Office Block, Hotel Equatorial Shanghai
No.65, Yan An Road (West), Shanghai, 200040, China
中国上海市延安西路65号上海国际贵都大饭店办公楼405单元
Phone: +86-21-62489820
Fax: +86-21-62489821

IntechOpen